Journal of Power Sources 244 (2013) 557–560

Contents lists available at SciVerse ScienceDirect

Journal of Power Sources

journal homepage: www.elsevier.com/locate/jpowsour

Short communication

Synthesis and lithium intercalation properties of Li_3VO_4 as a new anode material for secondary lithium batteries

Won-Tae Kim [a], Yeon Uk Jeong [a,*], Yong Joong Lee [b], Young Jun Kim [c], Jun Ho Song [c]

[a] School of Materials Science and Engineering, Kyungpook National University, Daegu 702-701, Republic of Korea
[b] School of Mechanical Engineering, Kyungpook National University, Daegu 702-701, Republic of Korea
[c] Advanced Batteries Research Center, Korea Electronics Technology Institute, Seongnam 463-816, Republic of Korea

HIGHLIGHTS

- Li_3VO_4 exhibits charge capacity of 190 mAh g^{-1}after 100th cycle.
- Average potential of Li_3VO_4 is lower than that of $Li_4Ti_5O_2$.
- Li_3VO_4synthesized by solution-based method shows an excellent cyclability.

ARTICLE INFO

Article history:
Received 24 September 2012
Received in revised form
15 January 2013
Accepted 28 January 2013
Available online 6 February 2013

Keywords:
Lithium-ion batteries
Anode materials
Lithium vanadium oxide
Crystal Structure
Electrochemical properties

ABSTRACT

Lithium intercalation properties of Li_3VO_4 are investigated for a possible application as a new anode material for lithium-ion batteries. A single phase Li_3VO_4 powders are successfully synthesized in an oxygen atmosphere by a two-step heating process and solution-based method. A structure with corner-shared VO_4 and LiO_4 tetrahedrons can reversibly intercalate lithium ions and exhibits a stable frame structure after cycling. The average discharge potential is lower than $Li_4Ti_5O_{12}$. While the sample obtained from the solid-state reaction shows initial instability and stabilizes by the continuous cycling, the sample synthesized by precipitation exhibits excellent cyclability. 190 mAh g^{-1} of charge capacity is observed after 100th cycle at 1.0 C-rate.

1. Introduction

Lithium-ion batteries have been commonly used in consumer electronics as well as in hybrid electric vehicles (HEVs). The next generation of secondary lithium batteries demands an enhanced energy density, rate capability, safety, cost, and environmental compatibility, etc. In this regard, oxide-based materials have been recently investigated for the anode of secondary lithium batteries. The spinel structure of $Li_4Ti_5O_{12}$ can intercalate three lithium ions per formula at the potential of 1.5 V vs. Li. Although the theoretical capacity is 175 mAh g^{-1}, 150–160 mA h g^{-1} of discharge capacity has been reported [1–5]. Good reversibility and no volume change during the intercalation process are achieved with $Li_4Ti_5O_{12}$. However, its demerits are the limited capacity and the relatively high potential as an anode material. While layered $Li_{1+x}V_{1-x}O_2$ ($0.075 \leq x \leq 0.1$) anode exhibits very high initial capacities at low potential (0.5–0.01 V vs. Li), its major difficulty for the anode application lies in the fast deterioration of the material [6–10].

So far, Li_3VO_4 has been studied for the preparation [11], crystal chemistry [11,12], single crystal growth [13,14], nonlinear optical materials for second harmonic generation (SHG) [15]. Because Li_3VO_4 is an ionic conductor as well as an electrical insulator, Li_3VO_4 material is considered as a solid electrolyte for lithium-ion batteries [16,17]. In this study, lithium intercalation properties of Li_3VO_4 are investigated as a new anode material for secondary lithium batteries. Results of X-ray diffraction, scanning electron microscopy (S.E.M.) observations, and electrochemical properties are reported.

2. Experimental

Li_3VO_4 samples are synthesized by two distinct methods: the solid-state reaction and the solution-based precipitation,

* Corresponding author. Tel.: +82 53 950 7586; fax: +82 53 950 5645.
E-mail address: jeong@knu.ac.kr (Y.U. Jeong).

0378-7753/$ – see front matter © 2013 Elsevier B.V. All rights reserved.
http://dx.doi.org/10.1016/j.jpowsour.2013.01.163

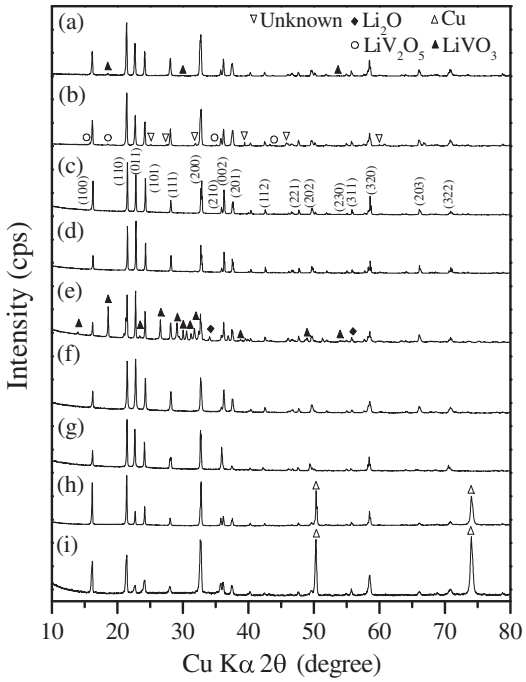

Fig. 1. X-ray powder diffraction patterns of various Li_3VO_4 samples (a) solid-state reaction with Li/V = 3.0 and heating at 1100 °C, (b) solid-state reaction with Li/V = 3.02 and heating at 1100 °C, (c) solid–state reaction with Li/V = 3.04 and heating at 1100 °C, (d) solid-state reaction with Li/V = 3.04 and heating at 700 °C, (e) solid-state reaction with Li/V = 3.04 and heating at 600 °C, (f) solution-based reaction, as-precipitated followed by heating at 500 °C, (g) solution-based reaction, as-precipitated sample, (h) as-pressed electrode (solid-state reaction at 1100 °C), (i) cycled electrode discharged at 2 V vs. Li after 30 cycles (solid-state reaction at 1100 °C).

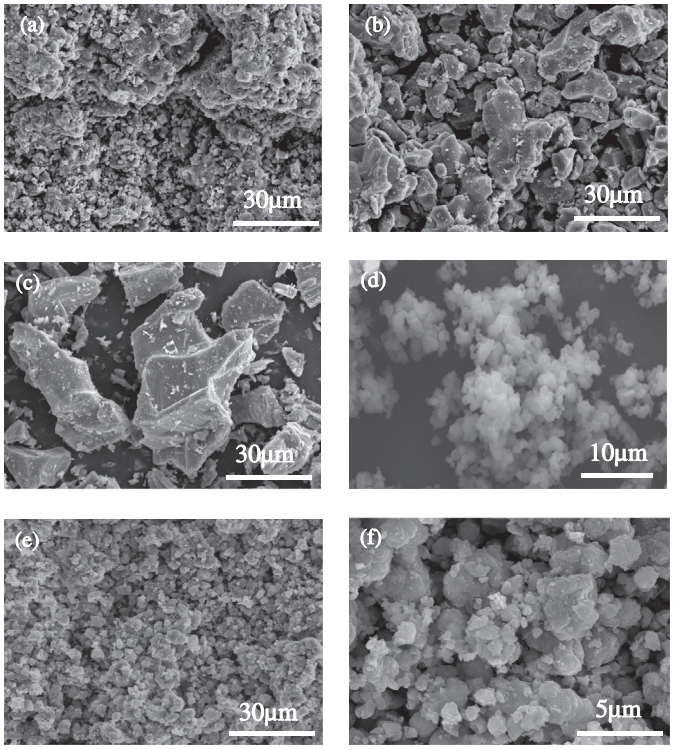

Fig. 2. S.E.M. pictures of various Li_3VO_4 samples (a) solid-state reaction with Li/V = 3.04 and heating at 700 °C, (b) solid-state reaction with Li/V = 3.04 and heating at 800 °C, (c) solid-state reaction with Li/V = 3.04 and heating at 1100 °C, (d) solution-based reaction, as-precipitated sample, (e) and (f) solution-based reaction, as-precipitated followed by heating at 500 °C.

respectively. In the case of the solid-state reaction, required amounts of Li_2CO_3 and V_2O_5 are mixed in a mortar for 1 h and pellets are prepared using mixed powders for the heat treatment. In order to identify a condition for obtaining a single phase product, Li/V ratios are controlled between 3 and 3.08. In order to avoid melting of V_2O_5 before the reaction with Li_2CO_3, pellets are heated in an oxygen atmosphere at 550 °C for 3 h and then heated at 600–1100 °C for 3 h to obtain the reaction products. For the precipitation from the aqueous solution, 25 ml of 3.04 M aqueous solution of LiOH is prepared by stirring for 1 h with a magnetic stirrer. 1 mol of V_2O_5 is mixed with aqueous LiOH and kept under constant stirring for 1 h to obtain a precipitated product. The product are then filtered and dried, followed by heating at 500 °C in air to remove the adsorbed water on the sample.

X-ray powder diffraction with X'Pert pro MPD (Cu Kα) and refinement are carried out to identify the phase and to determine the lattice constants, respectively. A field emission scanning electron microscope (FE-SEM, HITACHI S-4200) is used to observe the size and morphology of the powder sample. To identify the structural change of the cycled electrode, the electrode is carefully removed from the coin cell, and then washed with dimethyl carbonate (DMC) followed by drying in vacuum.

The electrochemical properties are evaluated by using coin cells (2032-type). The slurries are prepared by mixing of 80 wt% Li_3VO_4, 10 wt% Super P carbon as a conducting additive, 10 wt% polyvinylidene fluoride (PVDF) as a binder, and N-methyl pyrrolidone (NMP) as a solvent. Prepared slurries are coated onto a copper foil of 10 μm in thickness followed by drying in an oven at 120 °C and cold pressing. The loading in the electrode is 2.2–2.5 mg cm^{-2}. For electrolytes, 1 M $LiPF_6$is dissolved in the mixed solution of ethylene carbonate (EC) and ethyl methyl carbonate (EMC) with the ratio of 1:2. Lithium metal is used as the counter electrode and the coin cells are assembled in an Ar-filled glove box. The charge/discharge tests are performed between 2.0 and 0.1 V. Charge process is carried out by a constant current (0.2 C-rate), follow by a constant voltage (0.05 C-rate cut-off). Discharge is performed at 0.2, 0.5, and 1.0 C-rates and the current value for 1.0 C-rate is fixed at 100 mA g^{-1}. For cyclic voltammetry, the scan rate of 20 μV s^{-1} is applied between 2.0 V and 0.01 V.

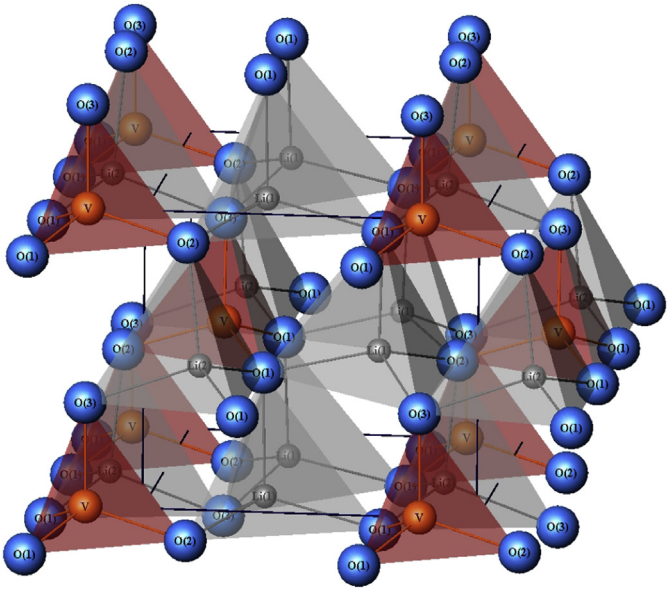

Fig. 3. Structure of the orthorhombic Li_3VO_4.

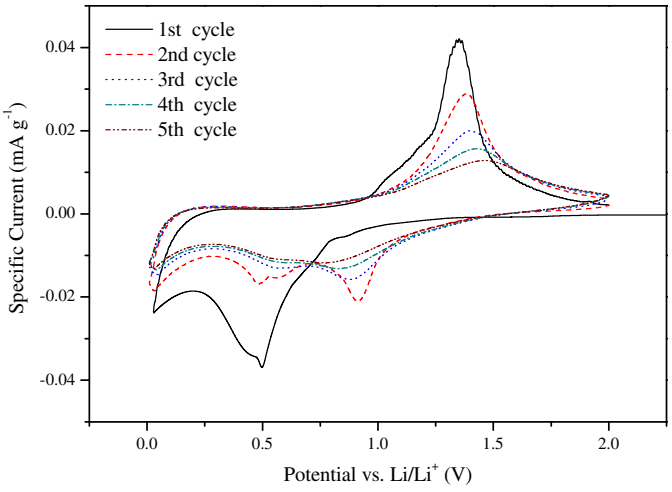

Fig. 4. Cyclic voltammograms of Li_3VO_4 anode with a scan rate of 20 μV s^{-1}.

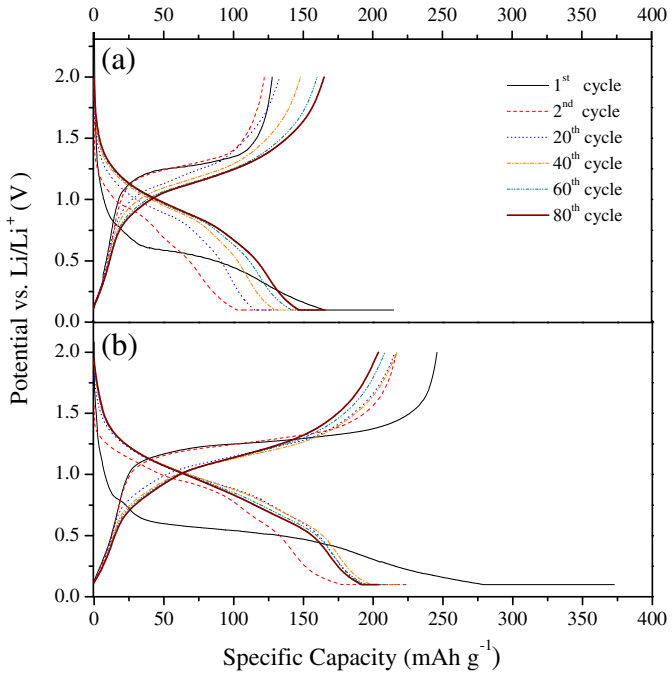

Fig. 5. Charge–discharge profiles of Li_3VO_4 anode at 0.2 C-rates (a) solid-state reaction with Li/V = 3.04 and heating at 1100 °C, (b) solution-based reaction, as-precipitated followed by heating at 500 °C.

3. Results and discussion

The results of X-ray powder diffraction for various samples are shown in Fig. 1. Various Li/V ratios are investigated for solid-state reaction. The samples with the Li/V ratios of 3.0 and 3.02 include $LiVO_3$, LiV_2O_5, or unknown impurities. As shown in Fig. 1(c), a single phase Li_3VO_4 is found for the Li/V ratio of 3.04, and synthesized Li_3VO_4 has a single phase of the orthorhombic structure with a space group of $Pnm2_1$ [11,12]. The effects of heating temperature of the second step are shown in Fig. 1(c)–(e). Reaction is not completed for the sample heated at 600 °C, but a single phase product can be obtained from the heating temperature of 700 °C. The sample heated at 1100 °C has the unit cell parameters and volume: *a*-axis = 5.444 Å, *b*-axis = 6.324 Å, *c*-axis = 4.947 Å, and 170.31 $Å^3$, respectively. In the case of solution-based synthesis, as shown in Fig. 1(f) and (g), as-precipitated sample has a good crystallinity similar to 500 °C heated sample. The unit cell volume decreases from 172.51 $Å^3$ to 170.63 $Å^3$ upon heating. Fig. 1(h) and (i) give XRD results of as-pressed electrode and cycled electrode discharged at 2 V vs. Li after 30 cycles. Although the peaks for the cycled electrode are slightly broadened, no new peaks have appeared indicating no newly formed phases upon cycling.

S.E.M. images of the samples synthesized by the solid-state reaction are shown in Fig. 2(a)–(c). Irregular agglomerates are observed in 700 °C heated sample. Particles tend to grow upon heating, and 1100 °C heated sample contains irregular shaped particles with the maximum size of ~30 μm. As shown in Fig. 2(d)–(f), 1–4 μm size individual particles are observed in the samples synthesized by the solution-based method.

As shown in Fig. 3, the structure of Li_3VO_4 is composed of corner-shared VO_4 and LiO_4 tetrahedrons. Lithium ions are expected to reversibly intercalate into empty sites in the structure. Although further oxidation of V^{5+} in Li_3VO_4 is hard to achieve, reduction to V^{4+} by the insertion of lithium in the structure is possible through the charging process. The result of cyclic voltammetry of Li_3VO_4 anode is shown in Fig. 4. The small reduction peak at ~0.85 V vs. Li in the first reduction cycle is related with the reduction of electrolyte [9]. This peak corresponds to the small inflections (0.75–0.8 V) in the first charge curves in Fig. 5(a) and (b), which show the charge and discharge profiles for the samples prepared by the solid–state reaction and the solution-based method, respectively. A large reduction peak at ~0.5 V vs. Li in the first reduction cycle in Fig. 4 corresponds to the plateaus in the first charge curves of Fig. 5(a) and (b). The average potential of the second charge curve is higher and decreases faster than the first charge curve. Two reduction peaks (0.47 V and 0.9 V vs. Li) in the second cycle are observed in Fig. 4, these two peaks correspond to the inflection points in the second charge curves in Fig. 5. However these two peaks eventually merged together upon further reduction process. This irreversible behavior of the first and second cycles in cyclic voltammetry is consistent with the result of the charge and discharge tests, this might be related with the intercalation instability at the initial stage.

Table 1
Charge/discharge capacities and efficiencies of various Li_3VO_4 samples.

Synthesis method	Cycle number	0.2 C-rate			0.5 C-rate			1.0 C-rate		
		Ch (mAh g^{-1})	Dch (mAh g^{-1})	Efficiency (%)	Ch (mAh g^{-1})	Dch (mAh g^{-1})	Efficiency (%)	Ch (mAh g^{-1})	Dch (mAh g^{-1})	Efficiency (%)
Solid-state reaction	1	214.86	127.81	59.48	182.56	91.59	50.16	184.22	75.95	41.23
	50	147.84	146.46	99.07	155.42	154.96	99.70	136.96	136.17	99.42
	100	164.84	163.68	99.30	179.23	177.78	99.19	179.67	179.19	99.73
Solution-based precipitation	1	372.75	245.63	65.90	344.20	229.78	66.76	361.22	249.14	68.97
	50	214.31	213.25	99.50	198.69	198.28	99.79	205.91	201.33	97.76
	100	197.97	196.86	99.44	186.49	184.62	98.99	190.65	185.55	97.32

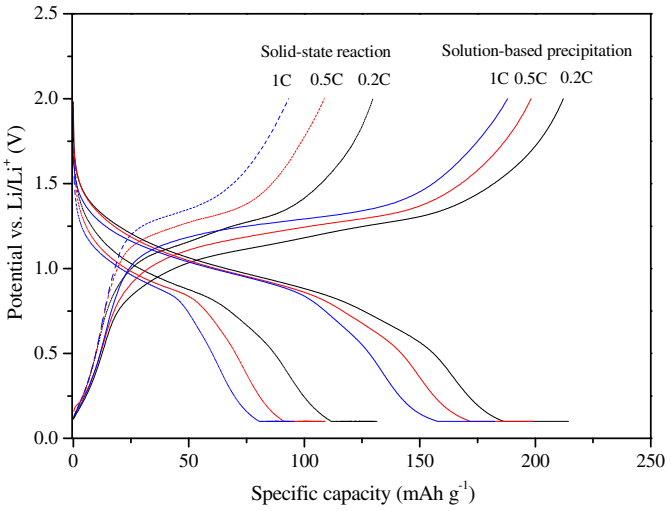

Fig. 6. Charge and discharge profiles of 10th cycle with various C-rates.

The results of the charge and discharge at 0.2 C-rate are shown in Fig. 5(a) and (b). The initial irreversibility might be due to the formation of SEI (solid electrolyte interphase) [6] as well as the irreversible reactions that include a reaction on the surface of Li_3VO_4 particles. As shown in Fig. 2, the sample prepared by solution-based method has a smaller average particle size than that heated at 1100 °C. Although the first charge and discharge exhibit a large irreversibility, the intercalation reaction in the electrode is eventually stabilized after the first cycle. The average potential for the discharge curves at 0.2 C-rates is found to be around 1.25 V and this potential is lower than that of $Li_4Ti_5O_{12}$. Charge and discharge capacities and coulombic efficiencies of various samples are summarized in Table 1. The coulombic efficiencies of samples with smaller particles are higher than those with larger particles. Charge and discharge profiles of 10th cycle of various C-rates are shown in Fig. 6. Higher rate capability is achieved for the precipitated samples with smaller particle sizes. Fig. 7 shows the cyclability data with various C-rates. While samples composed of small particles are stabilized after the first cycle, 1100 °C heated sample exhibits a slowly increasing capacity. This might be due to the slowly increasing diffusion distance in large particles upon cycling. This phenomenon is conspicuous for the higher C-rates. In the case of sample made by the solution-based process, the charge capacity of 190 mAh g^{-1} is obtained after 100th cycle with 0.2 C-rate charge and 1.0 C-rate discharge, and this corresponds to the insertion of 0.96 moles lithium in Li_3VO_4. The sample prepared by a precipitation followed by heating at 500 °C exhibits an excellent cyclability. The results of cyclability and XRD of cycled electrode possibly suggest the lithium intercalation reaction in Li_3VO_4 is reversible and the frame structure is stably maintained. The exact insertion sites for lithium in the unit cell and the effects upon doping with other metal ions will be investigated for the future research.

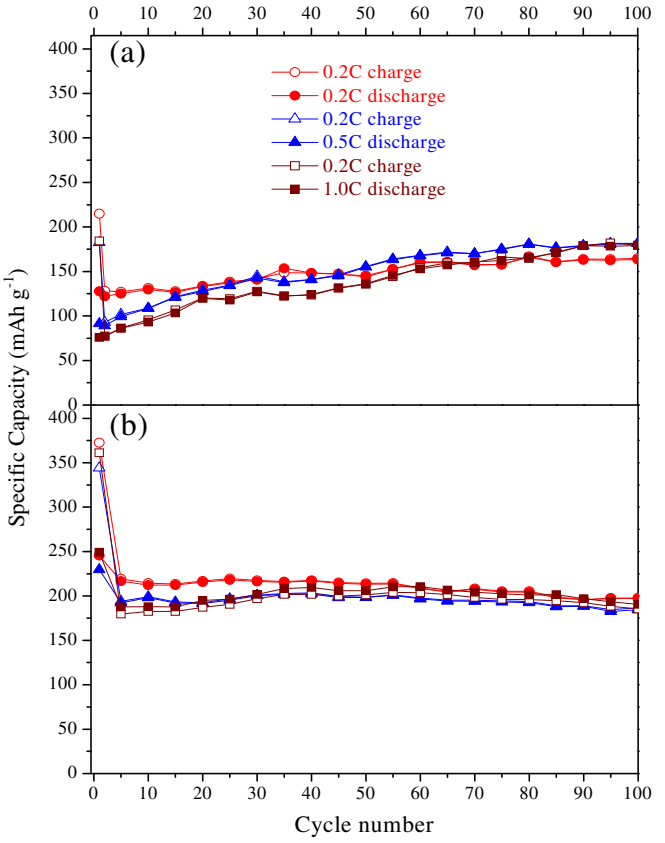

Fig. 7. Cyclabilities of Li_3VO_4 with various C-rates (a) solid-state reaction with Li/V = 3.04 and heating at 1100 °C, (b) solution-based reaction, as-precipitated followed by heating at 500 °C.

4. Conclusions

Li_3VO_4 powders are successfully synthesized by the solid-state reaction in the controlled atmosphere and by the solution-based reaction. Li_3VO_4 has a single phase of the orthorhombic structure with a space group of $Pnm2_1$. The average potentials of charge and discharge curves are lower than those of $Li_4Ti_5O_{12}$. Although the first charge and discharge exhibit irreversible capacities, the intercalation reactions are stabilized with cycling and excellent cyclabilities are achieved in Li_3VO_4 samples synthesized by the solution-based method. 190 mAh g^{-1} of charge capacity is observed after the 100th cycle and this corresponds to the insertion of 0.96 moles lithium in Li_3VO_4. Further investigations for improved performances are highly anticipated.

Acknowledgments

This work is supported by the Ministry of Knowledge Economy and KETEP (Korea Institute of Energy Technology Evaluation and Planning) for the development of materials and module of kWh-grade energy storage for the next generation.

References

[1] K.M. Colbow, J.R. Dahn, R.R. Haering, J. Power Sources 26 (1989) 397–402.
[2] K. Zaghib, M. Simoneau, M. Armand, M.J. Gauthier, J. Power Sources 81-82 (1999) 300–305.
[3] K. Nakahara, R. Nakajima, T. Matsushima, H. Majima, J. Power Sources 117 (2003) 131–136.
[4] K. Kanamura, T. Chiba, K. Dokko, J. Eur. Ceram. Soc. 26 (2006) 577–581.
[5] C. Jiang, Y. Zhou, I. Honma, T. Kudo, H. Zhou, J. Power Sources 166 (2007) 514–516.
[6] N.S. Choi, J.S. Kim, R.Z. Yin, S.S. Kim, Mater. Chem. Phys. 116 (2009) 603–606.
[7] J.H. Song, H.J. Park, K.J. Kim, Y.N. Jo, J.S. Kim, Y.U. Jeong, Y.J. Kim, J. Power Sources 195 (2010) 6157–6161.
[8] W.T. Kim, Y.U. Jeong, H.C. Choi, Y.J. Kim, J.H. Song, H. Lee, Y.J. Lee, J. Appl. Electrochem. 41 (2011) 803–808.
[9] A.R. Armstrong, C. Lyness, P.M. Panchmatia, M.S. Islam, P.G. Bruce, Nat. Mater. 10 (2011) 223–228.
[10] W.T. Kim, Y.U. Jeong, H.C. Choi, Y.J. Lee, Y.J. Kim, J.H. Song, J. Power Sources 221 (2013) 366–371.
[11] A.R. West, F.P. Glasser, J. Solid State Chem. 4 (1972) 20–28.
[12] R.D. Shannon, C.J. Calvo, J. Solid State Chem. 6 (1973) 538–549.
[13] S. Sakata, W. Itoyama, I. Fujii, K. Iishi, J. Cryst. Growth 135 (1994) 555–560.
[14] D.J. Kim, Y.-H. Hwang, H.K. Kim, J.N. Kim, Y. Kasuga, K.-I. Ohshima, J. Cryst. Growth 259 (2003) 115–120.
[15] S. Sakata, N. Ueda, I. Fujii, H. Kawazoe, J. Non-Cryst. Solids 178 (1994) 98–102.
[16] M. Touboul, A. Elfakir, M. Quarton, Solid State Ionics 82 (1995) 61–65.
[17] A. Kazakopoulos, O. Kalogirou, J. Mater. Sci. 44 (2009) 4987–4992.